



PERGAMON

International Journal of Solids and Structures 40 (2003) 701–714

INTERNATIONAL JOURNAL OF
SOLIDS and
STRUCTURES

www.elsevier.com/locate/ijsolstr

A combined approach of EFGM and precise algorithm in time domain solving viscoelasticity problems

Yang Haitian ^{*}, Liu Yan

*State Key Lab of Structural Analysis of Industrial Equipment, Department of Engineering Mechanics,
Dalian University of Technology, Dalian 116024, PR China*

Received 8 January 2002; received in revised form 9 October 2002

Abstract

In this paper, element free Galerkin (EFG) method is combined with a precise algorithm in the time domain for solving viscoelasticity problems. By expanding variables at discretized time intervals, an initial boundary value problem is converted into a series of recurrent boundary value problems which can be conveniently solved by EFG/EFG-FE with a self-adaptive computing process. There is no requirement of iteration for the solution of non-linear cases. Satisfactory numerical results are obtained for both static and dynamical viscoelasticity problems.

© 2002 Published by Elsevier Science Ltd.

Keywords: Precise algorithm in time domain; EFG method; Viscoelasticity

1. Introduction

Viscoelasticity is related with many engineering aspects. The activities in this field have been primarily due to the large scale development and utilization of polymeric materials (see e.g. Christensen, 1982).

The solution of viscoelasticity is time dependent. Due to the complexity of constitutive relationship, boundary condition and boundary geometry etc. although discretized in the space, numerical techniques are still required in the time domain for most cases.

For a specific discretized algorithm in the time domain, there are some decisive factors to be taken into account, such as consistency, convergence and stability. In addition to the above factors, the computing accuracy has to be considered. The computing accuracy is considerably affected by the size of time step that usually may hardly be predicted in many cases.

Yang (1999) presented a new precise algorithm in the time domain, which is self-adaptive for the change of the size of time step, and needs no iteration for the non-linear cases.

It is of interest to combine the above algorithm with the MESHLESS method, which has gained rapid development in recent years, and takes some advantages in solving boundary value problems (see e.g. Belytschko et al., 1994, 1996).

^{*}Corresponding author. Tel./fax: +86-411-4708393.

E-mail address: haitian@dlut.edu.cn (Y. Haitian).

In the field of numerical solution of viscoelasticity, a new attempt is made in this paper by combining the precise algorithm in the time domain with element free Galerkin method (EFGM) and a coupled element free Galerkin (EFG)-FE method. Numerical validations, including both static and dynamical cases, are presented with satisfactory results.

2. Recurrent governing equations

The governing equation of dynamical viscoelasticity problems can be described by (see e.g. Christensen, 1982)

$$\sigma_{ij,j} + B_i = \rho \frac{\partial^2 u_i}{\partial t^2} \quad x \in \Omega \quad (1)$$

$$\varepsilon_{ij} = \frac{1}{2}(u_{i,j} + u_{j,i}) \quad (2)$$

where $\sigma_{ij}(\mathbf{x}, t)$ and $\varepsilon_{ij}(\mathbf{x}, t)$ represent tensors of stress and strain, respectively, $u_i(\mathbf{x}, t)$ is the vector of displacement, $\rho(\mathbf{x})$ denotes the mass density, $B_i(\mathbf{x}, t)$ refers to body force, and Ω is the domain of the problem.

Summation convention is applied to subscribe j . For 2D problems, i, j range from 1 to 2, for 3D problems i, j range from 1 to 3.

The boundary is specified by

$$u_i = \tilde{u}_i \quad x \in \Gamma_u \quad (3)$$

$$\sigma_{ij} n_j = p_i = \tilde{p}_i \quad x \in \Gamma_\sigma \quad (4)$$

where n_j represents the unit outside normal, p_i refers to the vector of traction on the boundary, \tilde{u}_i, \tilde{p}_i are prescribed functions of u_i and p_i , $\Gamma = \Gamma_u + \Gamma_\sigma$ denotes the boundary of Ω , and subscripts u and σ denote stress and displacement, respectively.

Initial condition is

$$u_i = \tilde{u}_i^0 \quad \text{at } t = 0 \quad (5)$$

$$\frac{\partial u_i}{\partial t} = v_i = \tilde{v}_i^0 \quad \text{at } t = 0 \quad (6)$$

where $\tilde{u}_i^0(\mathbf{x})$ and $\tilde{v}_i^0(\mathbf{x})$ are prescribed functions.

The constitutive relationship of viscoelasticity is described by (see e.g. Yang, 2000)

$$\sigma_{ij} = F(\varepsilon_{lk}) \quad (7)$$

where $F(\varepsilon_{lk})$ is a prescribed function.

Within the time interval $t_0 \leq t \leq t_0 + T_s$, expanding all variables with term s then yields

$$\sigma_{ij} = \sum_{m=0} \sigma_{ij}^m s^m \quad (8)$$

$$\varepsilon_{ij} = \sum_{m=0} \varepsilon_{ij}^m s^m \quad (9)$$

$$B_i = \sum_{m=0} B_i^m s^m \quad (10)$$

$$u_i = \sum_{m=0}^{\infty} u_i^m s^m \quad (11)$$

$$\tilde{u}_i = \sum_{m=0}^{\infty} \tilde{u}_i^m s^m \quad (12)$$

$$p_i = \sum_{m=0}^{\infty} p_i^m s^m \quad (13)$$

$$\tilde{p}_i = \sum_{m=0}^{\infty} \tilde{p}_i^m s^m \quad (14)$$

where σ_{ij}^m , ϵ_{ij}^m , B_i^m , u_i^m , \tilde{u}_i^m , p_i^m and \tilde{p}_i^m represent expanding coefficients of σ_{ij} , ϵ_{ij} , B_i , u_i , \tilde{u}_i , p_i and \tilde{p}_i , respectively.

$$s = \frac{t - t_0}{T_s} \quad (15)$$

where t_0 and T_s refer to the initial point and size of the time interval, respectively.

By virtue of the chain rule

$$\frac{d}{dt} = \frac{d}{ds} \frac{ds}{dt} = \frac{1}{T_s} \frac{d}{ds} \quad (16)$$

$$\frac{d^2}{dt^2} = \frac{1}{T_s^2} \frac{d^2}{ds^2} \quad (17)$$

the first and second order derivatives of T with respect to t can be written as

$$\frac{\partial u_i}{\partial t} = \sum_{m=0}^{\infty} \frac{m+1}{T_s} u_i^{m+1} s^m \quad (18)$$

$$\frac{\partial^2 u_i}{\partial t^2} = \sum_{m=0}^{\infty} \frac{(m+2)(m+1)}{T_s^2} u_i^{m+2} s^m \quad (19)$$

Substitution of Eqs. (8)–(19) for Eqs. (1)–(4) then yields

$$\sigma_{ij,j}^m + B_i^m = \frac{(m+1)(m+2)}{T_s^2} \rho u_i^{m+2} \quad x \in \Omega \quad (20)$$

$$\epsilon_{ij}^m = \frac{1}{2}(u_{i,j}^m + u_{j,i}^m) \quad (21)$$

$$u_i^{m+2} = \tilde{u}_i^{m+2} \quad x \in \Gamma_u \quad (22)$$

$$\sigma_{ij}^m n_j = p_i^m = \tilde{p}_i^m \quad x \in \Gamma_\sigma \quad (23)$$

For a kind of viscoelastic materials, Eq. (14) can be written as (see e.g. Yang, 2000)

$$\sigma_{ij}^m = D_{ijkl} \sum_{n=0}^m c^{m,m-n} \epsilon_{kl}^{m-n} \quad (24)$$

where coefficient $c^{m,m-n}$ and tensor D_{ijkl} are constants.

3. Implementation of EFGM

By utilizing a weighing residual technique, Eqs. (20)–(24) can be written in a weak form (see e.g. Zienkiewicz and Morgan, 1983).

$$\int_{\Omega} \left(\sigma_{ij,j}^m + B_i^m - \rho \frac{(m+1)(m+2)}{T_s^2} u_i^{m+2} \right) u_i^* dv + \int_{\Gamma_u} (u_i^{m+2} - \tilde{u}_i^{m+2}) p_i^* d\Gamma - \int_{\Gamma_a} (p_i^m - \tilde{p}_i^m) u_i^* d\Gamma = 0 \quad (25)$$

where u_i^* and p_i^* are weighting functions.

The application of integral by parts for the above equation leads to

$$\begin{aligned} \frac{(m+1)(m+2)}{T_s^2} \int_{\Omega} u_i^{m+2} \rho u_i^* dv &= \int_{\Omega} B_i^m u_i^* dv + \int_{\Gamma_a} \tilde{p}_i^m u_i^* d\Gamma + \int_{\Gamma_u} p_i^m u_i^* d\Gamma + \int_{\Gamma_u} (u_i^{m+2} - \tilde{u}_i^{m+2}) p_i^* d\Gamma \\ &\quad - \int_{\Omega} \sigma_{ij}^m u_{i,j}^* dv \end{aligned} \quad (26)$$

By using EFG technique, u_i^m and u_i^* are approximated by

$$u_i^m = [\Phi] \{ \bar{u}_i^m \} \quad (27)$$

$$u_i^* = [\Phi] \{ \bar{u}_i^* \} \quad (28)$$

where $\{ \bar{u}_i^m \}$ and $\{ \bar{u}_i^* \}$ are the nodal vectors of u_i^m and u_i^* , respectively, and $[\Phi]$ represents a matrix of shape functions.

General nodal vectors are defined by

$$\{ \bar{u}^m \}^T = \left(\{ \bar{u}_1^m \}^T \quad \{ \bar{u}_2^m \}^T \quad \{ \bar{u}_3^m \}^T \right) \quad (29)$$

$$\{ \bar{u}^* \}^T = \left(\{ \bar{u}_1^* \}^T \quad \{ \bar{u}_2^* \}^T \quad \{ \bar{u}_3^* \}^T \right) \quad (30)$$

p_i^m and p_i^* can be interpolated along the boundary, having the form

$$p_i^m = [N] \{ \bar{p}_i^m \} \quad (31)$$

$$p_i^* = [N] \{ \bar{p}_i^* \} \quad (32)$$

where $[N]$ is a matrix of Lagrangian interpolating functions, $\{ \bar{p}_i^m \}$ and $\{ \bar{p}_i^* \}$ are the nodal vectors of p_i^m and p_i^* , respectively.

The general nodal vectors of $\{ \bar{p}_i^m \}$ and $\{ \bar{p}_i^* \}$ are defined by

$$\{ \bar{p}^m \}^T = \left(\{ \bar{p}_1^m \}^T \quad \{ \bar{p}_2^m \}^T \quad \{ \bar{p}_3^m \}^T \right) \quad (33)$$

$$\{ \bar{p}^* \}^T = \left(\{ \bar{p}_1^* \}^T \quad \{ \bar{p}_2^* \}^T \quad \{ \bar{p}_3^* \}^T \right) \quad (34)$$

Substituting Eqs. (29)–(34) for Eq. (26) with arbitrary $\{ \bar{u}^* \}^T$ and $\{ \bar{p}^* \}^T$ then yields

$$\begin{bmatrix} A_m & B_m \\ B_m^T & 0 \end{bmatrix} \begin{Bmatrix} \bar{u}^{m+2} \\ \bar{p}^m \end{Bmatrix} = \begin{Bmatrix} F_m \\ f_m \end{Bmatrix} \quad (35)$$

where

$$A_m = \frac{(m+1)(m+2)}{T_s^2} \int_{\Omega} [\Phi]^T \rho [\Phi] dv \quad (36)$$

$$F_m = \int_{\Omega} [\Phi]^T \{B^m\} dv + \int_{\Gamma_2} [\Phi]^T \{\tilde{p}^m\} dv - \int_{\Omega} [\Phi']^T \{\sigma^m\} dv \quad (37)$$

$$B_m = - \int_{\Gamma_u} [\Phi]^T [N] d\Gamma \quad (38)$$

$$f_m = - \int_{\Gamma_u} [N]^T \{\tilde{u}^{m+2}\} d\Gamma \quad (39)$$

where $[\Phi']$ represents a matrix of derivatives of $[\Phi]$.

By using Eq. (24), Eq. (37) can be expressed as

$$F_m = \int_{\Omega} [\Phi]^T \{B^m\} dv + \int_{\Gamma_2} [\Phi]^T \{\tilde{p}^m\} dv - \sum_{n=0}^m \left(\int_{\Omega} [\Phi']^T [C^{m,m-n}] [\Phi'] dv \right) \{\bar{u}^{m-n}\} \quad (40)$$

where matrix $[C^{m,m-n}]$ is associated with $c_{m,m-n}$ and D_{ijkl} .

For the case of static viscoelasticity problems, all the terms relevant to the dynamical effect need to be removed.

4. Coupled FE-EFG technique

Coupled EF-EFG schemes can be used to avoid inconvenience caused by dealing with essential boundary conditions via EFGM. Belytschko (see e.g. Belytschko, 1991, Belytschko et al., 1995) proposed a variational principle based coupling scheme which is rigorous and accurate, and can pass the patch test. In this paper, to simply illustrate the implementation combining coupled FE-EFG method with the precise algorithm, a coupling technique, which has been developed for the coupling boundary and finite element method (see e.g. Brebbia, 1984, Brebbia et al., 1984, Takao and Hidehero, 1988, Cox, 1988) is employed without constructing the interface element with hybrid displacement approximation in contrast to the scheme (see e.g. Belytschko et al., 1995).

Divide the whole domain into two parts, i.e. EFG domain, and FE domain where all the essential boundaries are assumed to be included.

In FE domain, a recurrent formula can be written as (Yang, 1999)

$$\frac{(m+1)(m+2)}{T_s^2} [M^{\text{FE}}] \{\bar{u}_{\text{FE}}^{m+2}\} = \{F_m^{\text{FE}}\} + \{f_m^{\text{FE}}\} - \sum_{n=0}^m [K_{m,m-n}^{\text{FE}}] \{\bar{u}_{\text{FE}}^{m-n}\} + [G] \{\bar{p}_i^m\} \quad (41)$$

where $\{\bar{u}_{\text{FE}}^m\}$ is a nodal vector of expanding coefficient of displacement, $\{\bar{p}_i^m\}$, unknown, refers to a nodal vector of expanding coefficient of traction on the interface.

$$[M^{\text{FE}}] = \sum_e \int_{\Omega_e} [N]^T \rho [N] dv \quad (42)$$

$$\{F_m^{\text{FE}}\} = \sum_e \int_{\Omega_e} [N]^T \{B^m\} dv \quad (43)$$

$$\{f_m^{\text{FE}}\} = \sum_e \int_{\Gamma_e} [N]^T \{\tilde{p}^m\} d\Gamma \quad (44)$$

$$[K_{m,m-n}^{\text{FE}}] = \sum_e \sum_{n=0}^m \int_{\Omega_e} [N']^T [C^{m,m-n}] [N'] dv \quad (45)$$

$$[G] = \sum_e \int_{\Gamma_i^e} [N]^T [N] d\Gamma \quad (46)$$

$[N]$ and $[N']$ denote matrixes of shape functions and their derivatives, respectively, summation \sum_e covers all finite elements.

Re-write Eq. (41) in the form

$$[A_m^{\text{FE}}] \{\bar{u}_m^{m+2}\} = \{b_m^{\text{FE}}\} + [G] \{\bar{p}_i^m\} \quad (47)$$

where

$$[A_m^{\text{FE}}] = \frac{(m+1)(m+2)}{T_s^2} [M^{\text{FE}}] \quad (48)$$

$$\{b_m^{\text{FE}}\} = \{F_m^{\text{FE}}\} + \{f_m^{\text{FE}}\} - \sum_{n=0}^m [K_{m,m-n}^{\text{FE}}] \{u_{\text{FE}}^{m-n}\} \quad (49)$$

By making use of

$$(p_i^m)^{\text{EFG}} = -(p_i^m)^{\text{FE}} = -[N] \{(\bar{p}_i^m)\}$$

Eq. (32) in the EFG domain can be rewritten as

$$\frac{(m+1)(m+2)}{T_s^2} [M^{\text{EFG}}] \{\bar{u}_{\text{EFG}}^{m+2}\} = \{F_m^{\text{EFG}}\} + \{f_m^{\text{EFG}}\} - \sum_{n=0}^m [K_{m,m-n}^{\text{EFG}}] \{\bar{u}_{\text{EFG}}^{m-n}\} - [J_{\text{EFG}}] \{\bar{p}_i^m\} \quad (50)$$

where $\{\bar{u}_{\text{EFG}}^m\}$ denotes the nodal vector of expanding coefficient of displacement, $\{p_i^m\}$ denotes the vector of traction on the interface, both subscripts and superscripts FE and EFG refer to EF domain and EFG domain, respectively.

$$[M^{\text{EFG}}] = \int_{\Omega_{\text{EFG}}} [\Phi]^T \rho [\Phi] dv \quad (51)$$

$$\{F_m^{\text{EFG}}\} = \int_{\Omega_{\text{EFG}}} [\Phi]^T \{B_m\} dv \quad (52)$$

$$\{f_m^{\text{EFG}}\} = \int_{\Gamma_i^{\text{EFG}}} [\Phi]^T \{\tilde{p}_m\} d\Gamma \quad (53)$$

$$[K_{m,m-n}^{\text{EFG}}] = \int_{\Omega_{\text{EFG}}} [\Phi']^T [C_{m,m-n}] [\Phi'] dv \quad (54)$$

$$[J_{\text{EFG}}] = \sum_e \int_{\Gamma_i^e} [\Phi]^T [N] d\Gamma \quad (55)$$

Eq. (50) can further be written as

$$[A_m^{\text{EFG}}] \{\bar{u}_{\text{EFG}}^{m+2}\} = \{b_m^{\text{EFG}}\} - [J_{\text{EFG}}] \{\bar{p}_i^m\} \quad (56)$$

where

$$[A_m^{\text{EFG}}] = \frac{(m+1)(m+2)}{T_s^2} [M^{\text{EFG}}] \quad (57)$$

$$\{b_m^{\text{EFG}}\} = \{F_m^{\text{EFG}}\} + \{f_m^{\text{EFG}}\} - \sum_{n=0}^m [K_{m,m-n}^{\text{EFG}}] \{\bar{u}_{\text{EFG}}^{m-n}\} \quad (58)$$

In the FE domain, separating the nodes at the interface from others then yields

$$\{\bar{u}_{\text{FE}}^m\}^T = \begin{pmatrix} \{\bar{u}_{\text{FE}}^m\}_a^T & \{\bar{u}_{\text{FE}}^m\}_b^T \end{pmatrix} \quad (59)$$

where subscripts b and a refer to the nodes at the interface and others else, respectively.

Since $[G]$ is only available at the interface Eq. (47) can be written in the form

$$\begin{bmatrix} (A_m^{\text{FE}})_{aa} & (A_m^{\text{FE}})_{ab} \\ (A_m^{\text{FE}})_{ba} & (A_m^{\text{FE}})_{bb} \end{bmatrix} \begin{Bmatrix} (\bar{u}_{\text{FE}}^{m+2})_a \\ (\bar{u}_{\text{FE}}^{m+2})_b \end{Bmatrix} = \begin{Bmatrix} (b_m^{\text{FE}})_a \\ (b_m^{\text{FE}})_b \end{Bmatrix} + \begin{bmatrix} 0 \\ G \end{bmatrix} \{\bar{p}_{\text{I}}^m\} \quad (60)$$

$\{\bar{p}_{\text{I}}^m\}$ can be obtained via Eq. (60), having the form

$$\{\bar{p}_{\text{I}}^m\} = [G]^{-1} \left([(A_m^{\text{FE}})_{ba}] \{(\bar{u}_{\text{FE}}^{m+2})_a\} + [(A_m^{\text{FE}})_{bb}] \{(\bar{u}_{\text{FE}}^{m+2})_b\} - \{(b_m^{\text{FE}})_b\} \right) \quad (61)$$

Substituting Eq. (61) for Eq. (56) with a rearrangement can yield

$$[A_m] \{\bar{u}^{m+2}\} = \{b_m\} \quad (62)$$

where

$$[A_m] = \begin{bmatrix} A_m^{\text{EFG}} + J_{\text{EFG}} J_{\text{FE}}^{-1} (A_m^{\text{FE}})_{bb} H & J_{\text{EFG}} J_{\text{FE}}^{-1} (A_m^{\text{FE}})_{ba} \\ (A_m^{\text{FE}})_{ab} H & (A_m^{\text{FE}})_{aa} \end{bmatrix} \quad (63)$$

$$\{b_m\} = \begin{Bmatrix} b_m^{\text{EFG}} + J_{\text{EFG}} J_{\text{FE}}^{-1} (b_m^{\text{FE}})_b \\ (b_m^{\text{FE}})_a \end{Bmatrix} \quad (64)$$

$$\{\bar{u}^{m+2}\}^T = \begin{pmatrix} \{\bar{u}_{\text{EFG}}^{m+2}\}^T & \{(\bar{u}_{\text{FE}}^{m+2})_a\}^T \end{pmatrix} \quad (65)$$

$$\{(\bar{u}_{\text{FE}}^m)_b\} = [H] \{\bar{u}_{\text{EFG}}^m\} \quad (66)$$

$$[H]^T = \begin{bmatrix} [\Phi]|_{\text{node } 1} & [\Phi]|_{\text{node } 2} & \dots & [\Phi]|_{\text{node } n_{\text{I}}} \end{bmatrix}^T \quad (67)$$

n_{I} is an integer representing the number of nodes at the interface.

5. Numerical validation

Example 1 (*Free vibration of a viscoelastic rod*). Consider a free vibration of a viscoelastic rod with $\rho = 100.0$ and $L = 0.9$.

A Kelvin model with $q_0 = 1.0$ and $q_1 = 2.0$, is used in the computation.

The initial condition is

$$u(x, 0) = \tilde{u}^0(x) = 0$$

$$\frac{\partial u(x, t)}{\partial t} \Big|_{t=0} = v(x, 0) = \tilde{v}^0(x) = 0.75 \frac{x}{L}$$

In the computing

$$T_s = 0.2 \text{ s}, \quad \beta = 1 \times 10^{-4}$$

15 equidistant nodes and two finite elements are employed.

Numerical comparisons with a FE based precise algorithm (see e.g. Gao, 1999) are exhibited from Figs. 2–6.

Example 2 (1D static viscoelastic problems). A viscoelastic rod, as shown in Fig. 1, is subjected to a load $P(t)$ at the right end. Various solutions of displacement are obtained for different constitutive models, and compared with analytical solutions (see e.g. Gao, 1999).

In the computing $\beta = 0.0001$.

The initial condition is

$$u(x, 0) = \tilde{u}^0(x) = 0$$

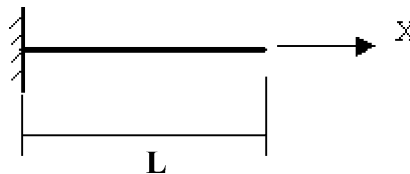


Fig. 1. A viscoelastic rod.

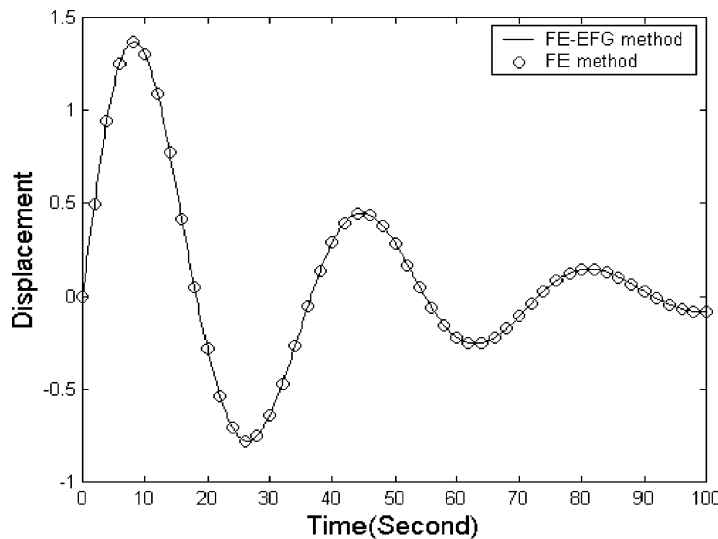
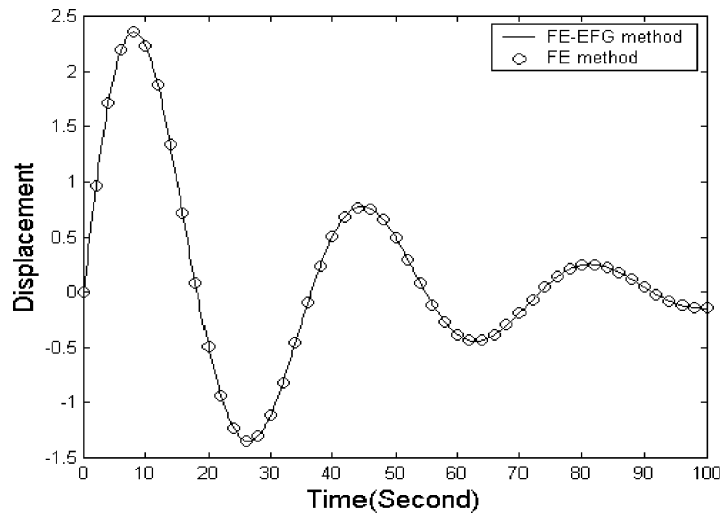
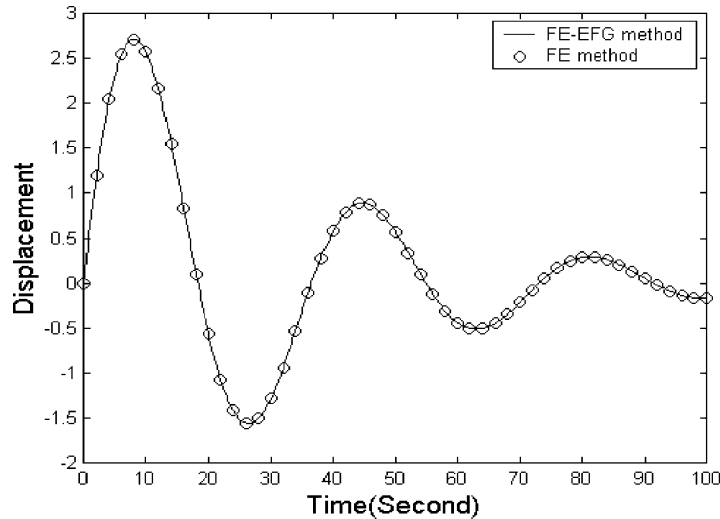


Fig. 2. Numerical comparison of displacement at $x = 0.3$.

Fig. 3. Numerical comparison of displacement at $x = 0.6$.Fig. 4. Numerical comparison of displacement at $x = 0.9$.

(1) *Linear model:*

$$P(t) = \begin{cases} 1.0 & 0 \leq t \leq 4.0 \\ 0 & t > 4.0 \end{cases}$$

Computing parameters are given in Table 1, numerical comparisons are exhibited in Table 2 and Fig. 7.
(2) *Linear model:*

$$P(t) = P_0 H(t)$$

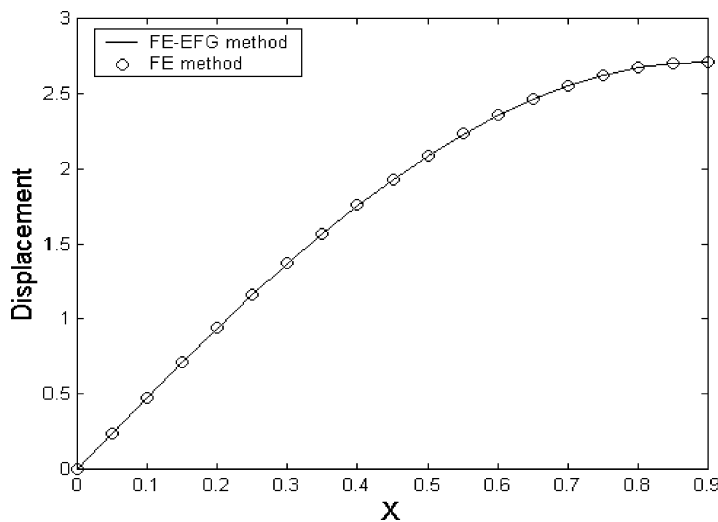
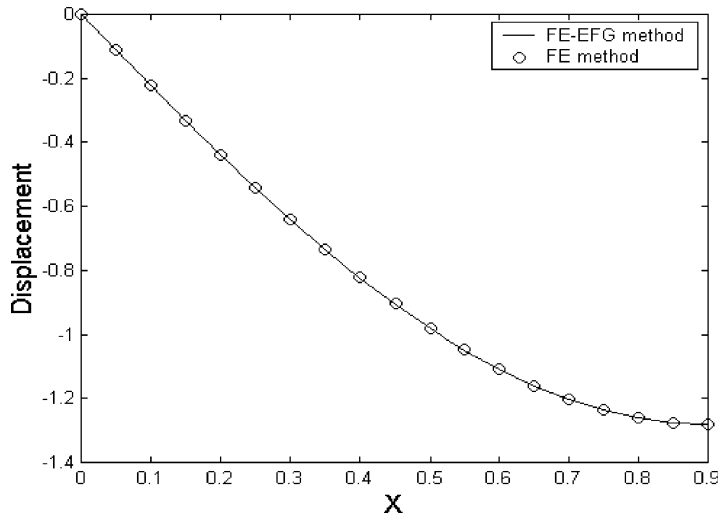
Fig. 5. Numerical comparison of displacement at $t = 8.2$ s.Fig. 6. Numerical comparison of displacement at $t = 30.0$ s.

Table 1
Computing parameters

Parameters	p_1	q_0	q_1	L	T_s	Number of nodes
Values	0.5	4×10^5	8×10^5	1.0	0.1	11

Table 2

Numerical comparison of displacement at $t = 3.0, 6.0$

x	$t = 3.0$		$t = 6.0$	
	Presented method (EFG)	Analytical solution	Presented method (EFG)	Analytical solution
0.2	4.1631E-07	4.1633E-07	1.1928E-007	1.1928E-007
0.5	1.0408E-06	1.0408E-06	2.9821E-007	2.9821E-007
0.7	1.4571E-06	1.4571E-06	4.1749E-007	4.1750E-007
0.9	1.8734E-06	1.8735E-06	5.3676E-007	5.3678E-007
1.0	2.0816E-06	2.0816E-06	5.9642E-007	5.9642E-007

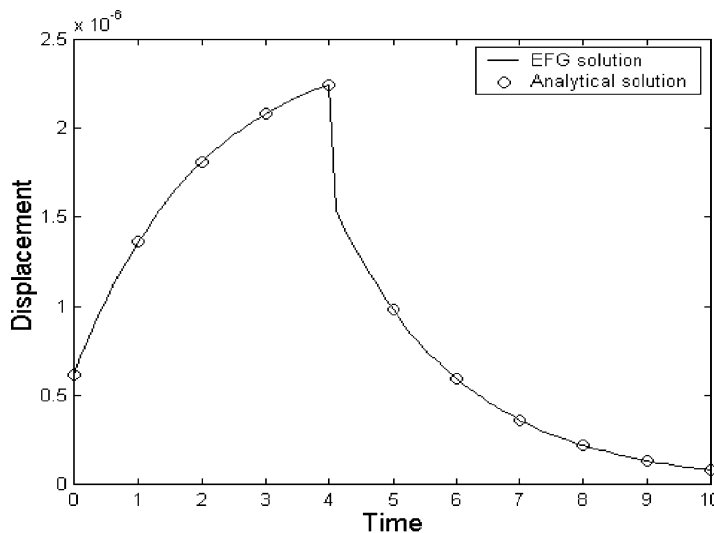
Fig. 7. Numerical comparison of displacement at $x = 0.9$.

Table 3

Computing parameters

Parameters	p_1	q_0	q_1	L	P	Number of nodes	Number of elements
Values	1.0	1.2×10^5	2.0×10^5	1.0	1000.0	10	1

where

$$H(t) = 0 \quad t < 0$$

$$H(t) = 1 \quad t \geq 0$$

Computing parameters are given in Table 3, numerical comparisons are shown in Tables 4 and 5.
(3) *Kelvin model*:

$$P(t) = P_0 H(t)$$

Computing parameters are listed in Table 6, numerical comparisons are exhibited in Tables 7 and 8.

Table 4

Numerical comparison of displacement at $x = 1.0, 0.7$

x	Size of time step	t	Presented method (EFG-FE)	Analytical solution
1.0	0.1	0.1	5.1941E-003	5.1941E-003
		0.2	5.3769E-003	5.3769E-003
		0.3	5.5491E-003	5.5491E-003
		0.4	5.7112E-003	5.7112E-003
		0.5	5.8639E-003	5.8639E-003
	0.5	0.5	5.8639E-003	5.8639E-003
		1.0	6.5040E-003	6.5040E-003
		1.5	6.9781E-003	6.9781E-003
		2.0	7.3293E-003	7.3294E-003
		2.5	7.5895E-003	7.5896E-003
0.7	0.2	0.2	3.7638E-003	3.7639E-003
		0.4	3.9979E-003	3.9979E-003
		0.6	4.2054E-003	4.2054E-003
		0.8	4.3895E-003	4.3895E-003
		1.0	4.5528E-003	4.5528E-003
	0.4	0.4	3.9978E-003	3.9979E-003
		0.8	4.3895E-003	4.3895E-003
		1.2	4.6975E-003	4.6976E-003
		1.6	4.9399E-003	4.9399E-003

Table 5

Numerical comparison of displacement at $t = 5.0$

Size of time step	x	Presented method (EFG-FE)	Analytical solution
5.0	0.2	1.6338E-003	1.6335E-003
	0.4	3.2670E-003	3.2670E-003
	0.6	4.9004E-003	4.9004E-003
	0.8	6.5339E-003	6.5339E-003
	1.0	8.1673E-003	8.1674E-003

Table 6

Computing parameters

Parameters	q_0	q_1	L	P	Number of nodes	Number of elements
Values	5.0×10^5	2.4×10^5	1.0	4000.0	10	1

Table 7

Numerical comparison of displacement at $x = 0.5, 0.8$

x	Size of time step	t	Presented method (EFG-FE)	Analytical solution
0.5	0.3	0.3	1.8590E-003	1.8590E-003
		0.6	2.8540E-003	2.8540E-003
		0.9	3.3866E-003	3.3866E-003
		1.2	3.6716E-003	3.6717E-003
		1.5	3.8243E-003	3.8243E-003
0.8	0.9	0.9	5.4186E-003	5.4185E-003
		1.8	6.2495E-003	6.2495E-003
		2.7	6.3769E-003	6.3769E-003
		3.6	6.3966E-003	6.3965E-003

Table 8
Numerical comparison of displacement at $t = 3.0$

Size of time step	x	Presented method (EFG-FE)	Analytical solution
3.0	0.1	7.9847E-004	7.9846E-004
	0.3	2.3953E-003	2.3954E-003
	0.5	3.9923E-003	3.9923E-003
	0.7	5.5893E-003	5.5892E-003
	0.9	7.1859E-003	7.1861E-003

6. Conclusions

The major objective of this paper is to make a new attempt combining EFGM with a precise algorithm in the time domain to solve viscoelasticity problems, the merits of this combination include

1. An initial boundary value problem is converted into a series of recurrent boundary value problems which are solved by EFGM as in the case of static elasticity. In addition to EFGM, other well developed numerical approaches can also be adopted with a specific consideration of characteristics of the problem, including in-homogeneity, complex boundary shape, and boundary conditions etc.
2. A self-adaptive computation can be realized by using the precise algorithm in the time domain, which results in a more precise description for the variation of variables, and compensates the possible lost computing accuracy caused by improper choices of the size of time step.
3. For non-linear cases, no any assumption is made, and no any iteration is needed.
4. By utilizing a coupling technique developed for the coupling FE-BE method, the implementation combining coupled FE-EFG methods with the precise algorithm in time domain is simply illustrated. Mathematically Eqs. (20)–(24) can also definitely be solved via the coupling approach proposed by Belytschko (see e.g. Belytschko, 1991, Belytschko et al., 1995), which is more accurate than the coupling technique used in this paper (see e.g. Belytschko, 1991), and is being employed by authors for solving 2D viscoelasticity problems with an expectation of more perfect results.

Numerical validation, including both static and dynamical cases, presents a good accordance with other solutions, which do encourage authors to extend present work to other fields. In fact, some preliminary results have been achieved for the solutions of heat conduction problems, and will be presented somewhere else.

Acknowledgements

The research leading to this paper is funded by the oversea returnee's initiating fund (1999-363), the key project fund (99149), and backbone faculty fund (2000-65), all of which came from National Education Department of PR China. The research is also funded by opening fund of State Key Lab of Structural Analysis of Industrial Equipment (GZ9814), NKBRSP (G1999032805), Key project fund of NSF (10032030), and NSF (10172024).

Thanks go to Prof. D.A. Tortorelli, and Department of Mechanical and Industrial Engineering, University of Illinois at Urbana and Champaign, USA for their providing all convenience to complete the framework of this article.

References

Belytschko, T., 1991. Singular integration in variationally coupled FE-BE. *Journal of Engineering Mechanics-ASCE* 117 (4), 830–835.

Belytschko, T., Lu, Y.Y., Gu, L., 1994. Element free Galerkin methods. *International Journal for Numerical Methods in Engineering* 37, 229–256.

Belytschko, T., Organ, D., Krongauz, Y., 1995. A coupled finite element–element free Galerkin method. *Computational Mechanics* 17, 186–195.

Belytschko, T., Krongauz, Y., Organ, D., et al., 1996. Meshless methods: an overview and recent developments. *Computer Methods in Applied Mechanics and Engineering* 139, 3–47.

Brebbia, C.A., Telles, J.C.F., Wrobel, L.C., 1984. *Boundary Element Techniques*. Springer-Verlag, Berlin, Heidelberg.

Brebbia, C.A., 1984. Boundary Elements. In: *Mathematical and Computational Aspects*, vol. 1. Springer-Verlag, Berlin, Heidelberg.

Christensen, R.M., 1982. *Theory of Viscoelasticity*. Academic Press, New York.

Cox, J.V., 1988. Coupling of the finite and boundary element methods in elastostatics, TN-1790. Naval Civil Engineering Laboratory.

Gao, Q., 1999. A precise algorithm in time domain to solve the problem of heat transfer. Bachelor Thesis, Dalian University of Technology.

Takao, S., Hidehero, S., 1988. Indentation by circular punch with BEM/FEM combination analysis. In: *Proceedings of the 2nd China-Japan Symposium on Boundary Elements*. Beijing, pp. 329–336.

Yang, H., 1999. A new approach of time stepping for solving transfer problems. *Communications in Numerical Method in Engineering* 15, 325–334.

Yang, H., 2000. Perturbation boundary-finite element combined method for solving the linear creep problem. *International Journal of Solids and Structures* 37, 2167–2183.

Zienkiewicz, O.C., Morgan, K., 1983. *Finite Elements and Approximation*. John Wiley & Sons, USA.